

AgRP neurons regulate development of dopamine neuronal plasticity and non food-associated behaviors

Marcelo O. Dietrich^{1,6}, Jeremy Bober¹, Jozélia G. Ferreira^{4,5}, Luis A. Tellez^{4,5}, Yann Mineur⁴, Diogo O. Souza⁶, Xiao-Bing Gao¹, Marina Picciotto⁴, Ivan Araújo^{4,5}, Zhong-Wu Liu¹ and Tamas L. Horvath^{1,2,3}

¹Program in Integrative Cell Signaling and Neurobiology of Metabolism, Section of Comparative Medicine and Departments of ²Obstetrics, Gynecology and Reproductive Sciences, ³Neurobiology and ⁴Psychiatry, Yale University School of Medicine, New Haven CT 06520, USA. ⁵The John B. Pierce Laboratory, New Haven CT 06520, USA.

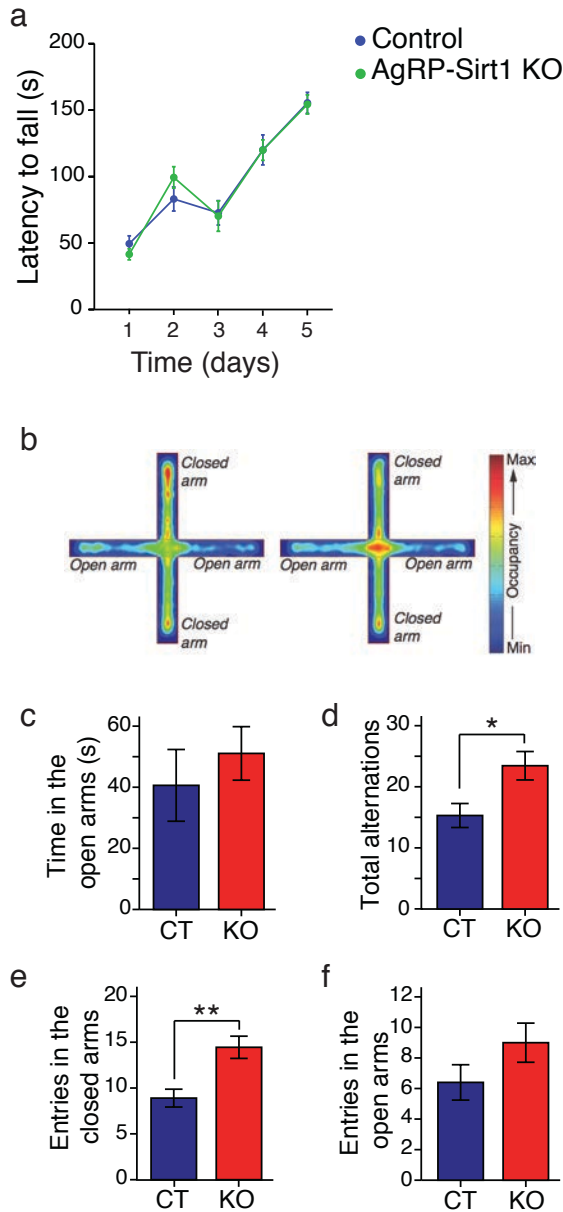
⁶Department of Biochemistry, Universidade Federal do Rio Grande do Sul, Porto Alegre RS 90035, Brazil.

Correspondence and requests for materials should be addressed to T.L.H.
(tamas.horvath@yale.edu).

Supplementary Figures 1-8.

Supplementary Tables 1-2.

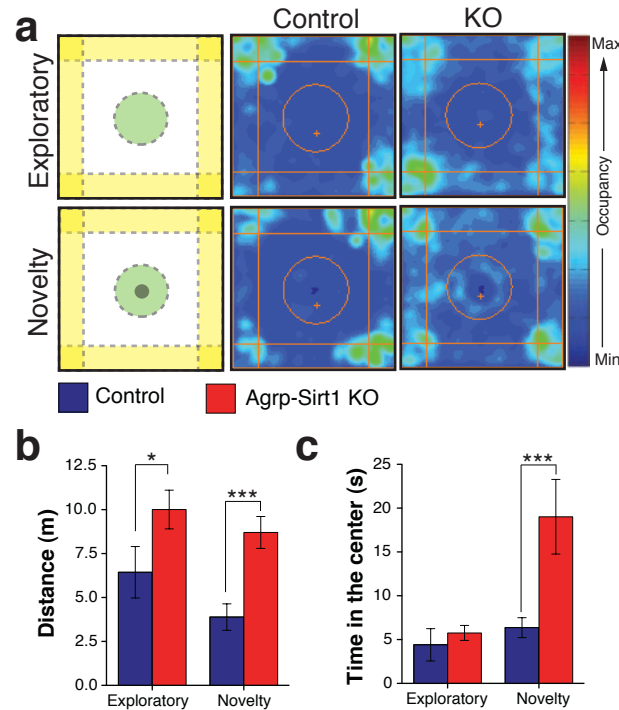
Supplementary Figure 1:



Motor coordination and anxiety trait in control and AgRP-Sirt^{-/-} mice.

(a) Rota-rod performance of control ($n = 12$) and AgRP-Sirt1^{-/-} ($n = 12$) female mice. Both groups of mice presented similar latency to fall off the rota-rod and similar learning curves during the 5 days of experiments ($\epsilon = 0.603$; time: $F_{(2,412, 53.064)} = 55.847$, $P < 0.001$; time x genotype: $F_{(2,412, 53.064)} = 0.555$, $P = 0.610$; genotype: $F_{(1, 22)} = 0.004$, $P = 0.948$). These data reinforce the changes in activity observed in the AgRP-Sirt1 KO mice and are not related to changes in motor coordination or motor learning skills. **(b-f)** AgRP-Sirt1^{-/-} mice did not display changes in anxiety in the plus-maze test. **(b)** Occupancy plots of the averaged position of the body of littermate controls (left) and AgRP-Sirt1^{-/-} mice (right) in a plus-maze test. Mice tend to spend the majority of their time in the closed arms and in the center of the apparatus, while making some attempts to explore the open arms. **(c)** The time spent in the open arms was not significantly different between controls and AgRP-Sirt1^{-/-} mice. **(d)** AgRP-Sirt1^{-/-} mice explore the apparatus more as measured by the number of alternations, which was mainly due to alternations in the closed arms **(e)**, but not into the open arms **(f)**. * $P < 0.05$, ** $P < 0.01$. Control ($n = 10$) and AgRP-Sirt1^{-/-} ($n = 9$). Bars represent mean \pm s.e.m.

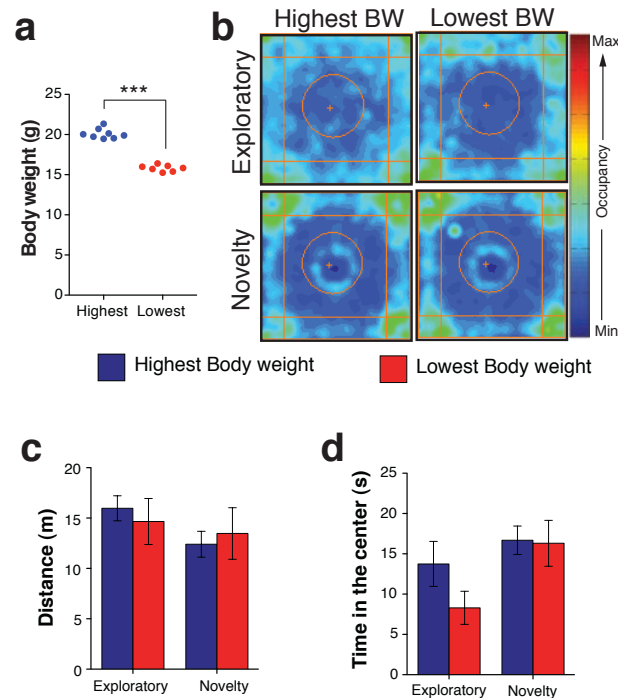
Supplementary Figure 2:



Leptin replacement did not revert the response of AgRP-Sirt1^{-/-} mice to novelty.

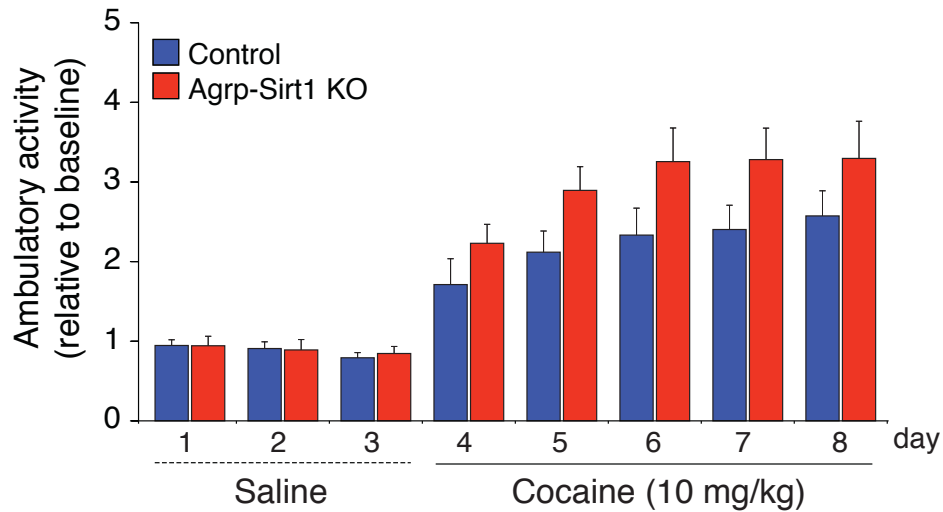
The altered excitability of the AgRP neurons in the AgRP-Sirt1^{-/-} mice leads to decreased adiposity, and an expected decrease in blood leptin levels (Supplementary Table 1). Leptin has been shown to directly modulate the VTA dopamine neuronal activity, and locomotor activity in mice. Thus, one possibility is that the decreased leptin levels in the AgRP-Sirt1 KO mice could lead to the behavioral alterations in the response of these mice to novelty. We replaced leptin in the AgRP-Sirt1 KO mice, and we found no changes in the behavioral response to novelty. The same mice tested in Figure 1 (main text), were re-tested in the open-field after an injection of leptin (5 mg/kg, i.p.). **(a)** Occupancy plots of the average position of the head for each group during both exploratory (no object) and novelty (novel object in the center) stages. **(b)** AgRP-Sirt1 KO mice show increased exploratory activity in the open-field, and **(c)** spent more time in the center of the arena when the object was inserted as a stimulus. * $P < 0.05$, *** $P < 0.001$. Control (n = 10) and AgRP-Sirt1^{-/-} (n = 9). Bars represent mean \pm s.e.m.

Supplementary Figure 3:



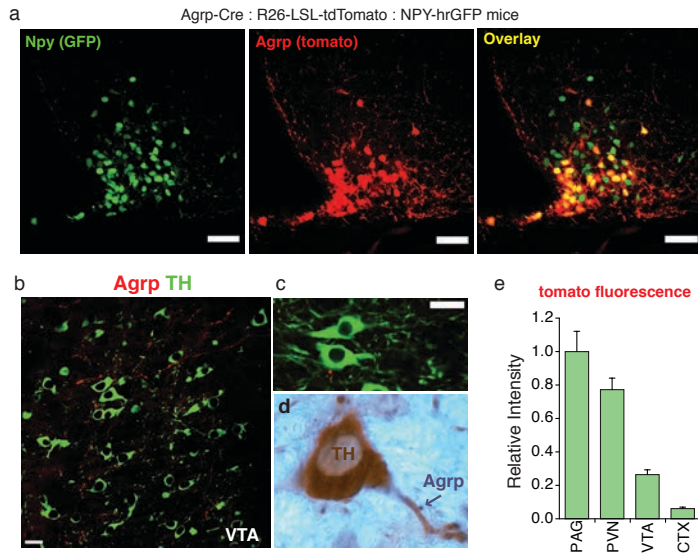
Mice selected to show natural differences in body weight have similar response to novelty in the open-field test. We selected mice with high and low body weights from a pool of 40 random C57B6/J female mice, to test whether the differences in body weight and adiposity between control and AgRP-Sirt1^{-/-} mice could be mimicked in mice that show natural differences in body mass. **(a)** Differences in body weight between the two groups. **(b)** Occupancy plots of the average position of the head for each group during both exploratory (no object) and novelty (novel object in the center) stages. **(c)** No differences were observed between the two groups in the exploratory activity in the open-field, and **(d)** in the time spent in the center of the arena. *** $P < 0.001$. Lowest BW ($n = 7$) and Highest BW ($n = 8$). Bars represent mean \pm s.e.m.

Supplementary Figure 4:



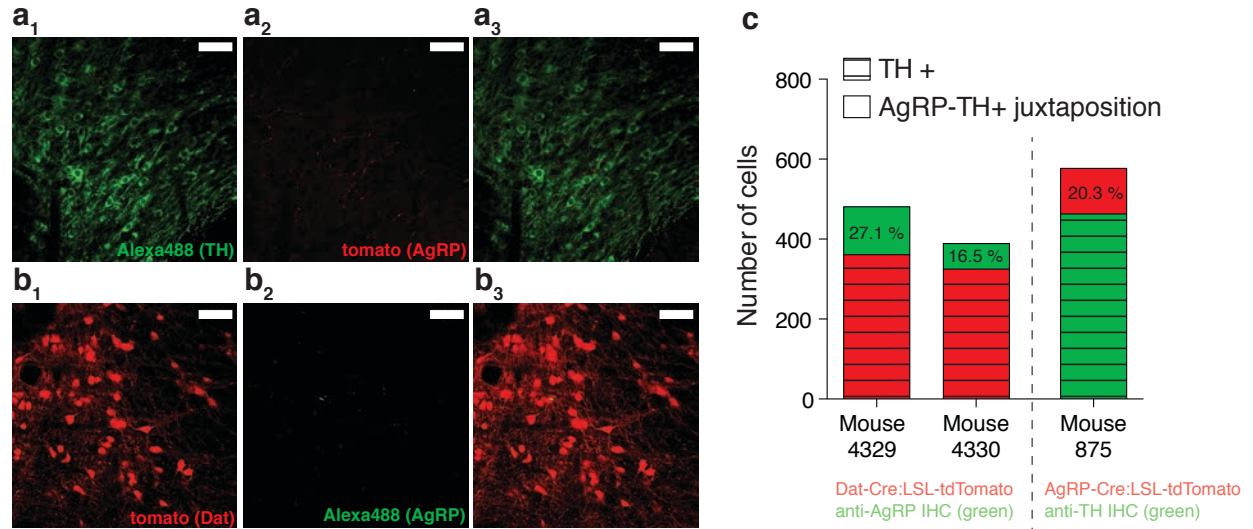
Response of control and AgRP-Sirt1^{-/-} to a cocaine sensitization protocol. Control and AgRP-Sirt1^{-/-} were challenged with saline or cocaine injections to induce locomotor sensitization. Despite a higher baseline activity (day 0 – data not shown), these mice did not show any major differences in their response to saline or cocaine treatments, as measured by relative changes related to baseline activity (day 0). Mice were first acclimated in the locomotor activity chamber for 60 minutes on day 0 (data not shown). On days 1-3, all mice received a saline injection (i.p.) and their activity was recorded for 20 minutes (data are related to individual mouse locomotor activity on day 0 to normalize for differences in baseline activity). There was no difference in the locomotor response to saline acclimation between control and AgRP-Sirt1^{-/-} mice (time: $F_{(2, 42)} = 3.694$, $P = 0.033$; time x genotype: $F_{(2, 42)} = 0.325$, $P = 0.725$; genotype: $F_{(1, 21)} = 0.008$, $P = 0.930$). From days 4-8, mice received one daily injection of cocaine (10 mg/kg, i.p.) to elicit sensitization of their locomotor response. Both control and AgRP-Sirt1^{-/-} mice had a similar response to the cocaine sensitization protocol ($\epsilon = 0.493$; time: $F_{(1.974, 41.453)} = 11.966$, $p < 0.001$; time x genotype: $F_{(1.974, 41.453)} = 0.490$, $P = 0.613$; genotype: $F_{(1, 21)} = 3.035$, $P = 0.096$). Next, cocaine treatment was withdrawn for 4 days, and all mice were challenged with saline on day 13 and cocaine on day 14 to test for contextual and drug sensitization respectively (see Fig. 1).

Supplementary Figure 5:



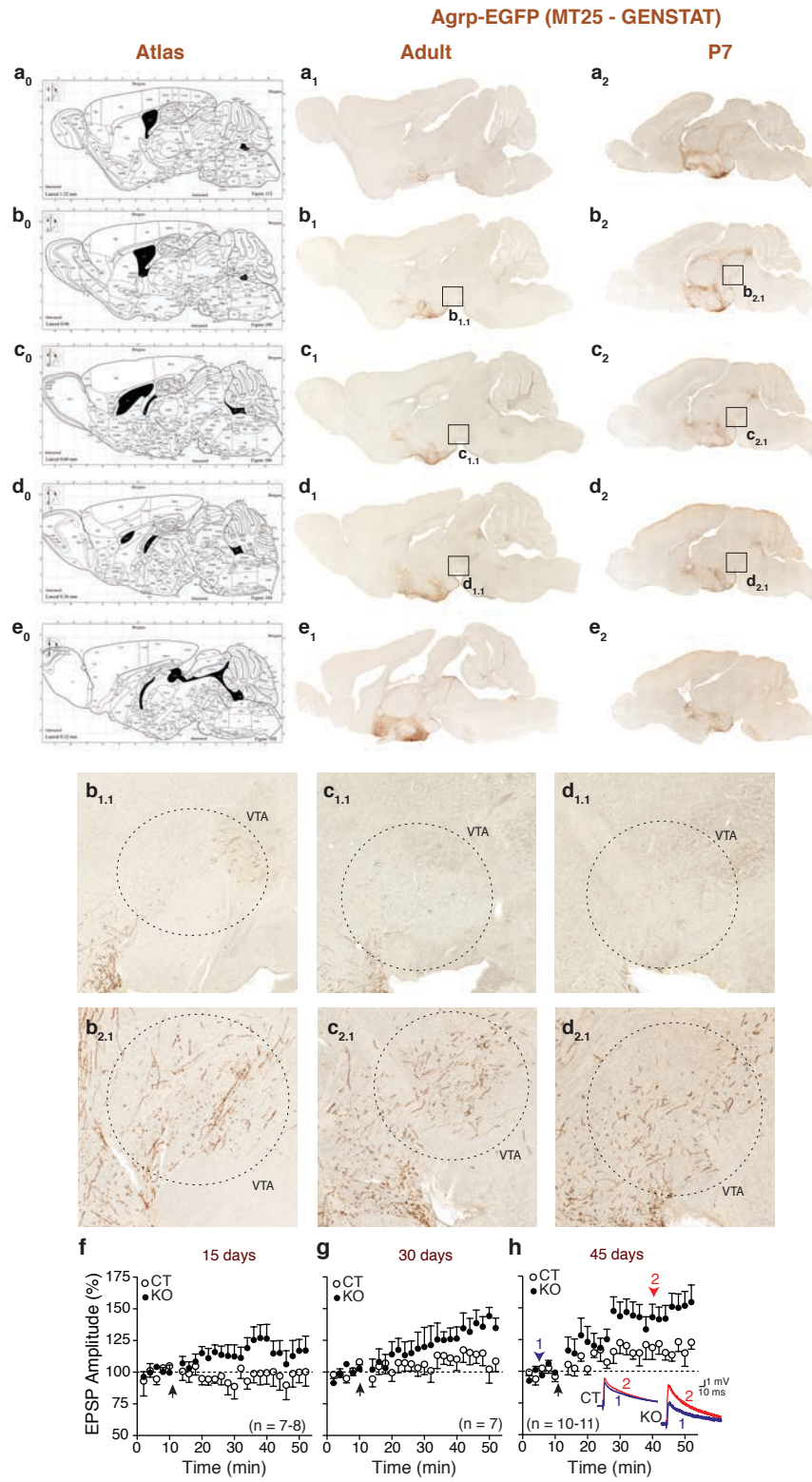
(a) Characterization of AgRP-Cre:R26-LSL-tdTomato:hrNPY-GFP reporter mice. Transgenic mice expressing Cre recombinase in AgRP neurons were crossed with mice carrying the reporter Rosa26-loxP-STOP-loxP-tdTomato allele and the NPY-hrGFP reporter transgene. *Left panel*, GFP fluorescence labeling of NPY neurons in the ARC. *Middle panel*, tdTomato fluorescence labeling of AgRP neurons. *Right panel*, overlay showing in yellow the neurons that co-express NPY/AgRP and a population of neurons that express NPY but do not express AgRP. Scale bars = 50 μ m. **(b-e)** AgRP neurons from the ARC nucleus send weak to moderate projections to the VTA. **(b)** Confocal scan from the VTA of AgRP-Cre:R26-LSL-tdTomato mice, showing AgRP fibers (red) located in the vicinity of the dopamine cells (green – TH immunostaining). **(c)** Close-up showing an AgRP terminal in close proximity to the TH neuron. **(d)** Double-immunohistochemistry showing AgRP terminals (Nickel-DAB – bluish) in close proximity to TH neurons (regular DAB – brownish). **(e)** Quantification of red fluorescence intensity in diverse brain areas of AgRP-Cre:R26-LSL-tdTomato mice. Altogether, the available data suggest that there is a direct innervation of the DA cells in the VTA by AgRP fibers. The moderate innervation of the VTA by AgRP fibers resembles that of orexin/hypocretin innervations of the same brain region. Orexin neurons projecting from the lateral hypothalamus have a major impact on the dopaminergic system within the VTA, and consequent behavior. Unexpectedly, the orexin projecting fibers to the VTA are sparse and synapse infrequently in this area. Thus, even though the AgRP neurons do not project massively to the VTA, it is not unlikely that they promote an important neurobiological effect on this region.

Supplementary Figure 6:



AgRP neuronal fibers from the ARC are juxtaposed to dopamine cells in the VTA. We used Dat-Cre:R26-LSL-tdTomato and AgRP-Cre:R26-LSL-tdTomato combined with IHC to track the interaction of AgRP fibers with dopamine neurons in the VTA. **(a)** Slice containing the VTA of AgRP-Cre:R26-LSL-tdTomato mice stained against TH and labeled with Alexa488 secondary antibody. **(a₁)** Green channel (Alexa488) showing TH+ neurons in the VTA; **(a₂)** red channel showing endogenous tomato fluorescence from the AgRP fibers; **(a₃)** merged channel. **(b)** Slice containing the VTA of Dat-Cre:R26-LSL-tdTomato mice stained against AgRP and labeled with Alexa488 secondary antibody. **(b₁)** red channel showing endogenous tomato fluorescence from the dopamine neurons in the VTA and their fibers; **(b₂)** green channel showing AgRP fibers innervating the VTA of adult mice, as labeled by an antibody against AgRP and a secondary antibody coupled to Alexa488; **(b₃)** merged channel. **(c)** Quantification of the interaction (close proximity) between AgRP fibers and dopamine cells in the VTA from three mice. More than 1400 dopamine cells were visualized, and – on average – at least 1 interaction every 6 cells was seen in a 40x confocal slice of the VTA of adult mice. Scale bars = 50 μ m.

Supplementary Figure 7:



Legend for Supplementary Figure 7:

AgRP projections to the VTA and LTP propagation in dopamine cells from the

VTA during development (a-e) Sagittal slices of the mouse brain showing the

localization of AgRP. These images correspond to a transgenic mouse generated by the GENSTAT Project, in which EGFP is expressed under the promoter of AgRP (AgRP-

EGFP mouse line – MT25). The brain is stained against GFP and developed with DAB.

(a-e₀) Sagittal slices from the adult mice Paxinus brain atlas. **(a-e₁)** Slices from adult

AgRP-EGFP mice, and **(a-e₂)** from postnatal day 7 (P7) mice. **(b-d_{1,1})** show inserts from

adult mice VTA, and **(b-d_{2,1})** show inserts from P7 mice VTA. While there is a weak to

moderate innervation of the VTA by AgRP fibers in adult mice, there is a strong

innervation of this midbrain nucleus in P7 mice. These images are courtesy of NCBI, and

are found online in the GENSTAT database – “The Gene Expression Nervous System

Atlas (GENSAT) Project, NINDS Contracts N01NS02331 & HHSN271200723701C to

The Rockefeller University (New York, NY)”. See Gong, S., et al. Nature 425, 917-925

(2003). **(f-h)** In the presence of a GABA_A blocker, STD-LTP protocol was applied to **(f)**

15-day-old, **(g)** 30-day-old, and **(h)** 45-day-old control and AgRP-Sirt1 KO mice. AgRP-

Sirt1 KO mice displayed enhanced LTP facilitation compared to control mice, as early as

15 days of age. A summary of this data is in **Fig. 2f** (main text). In **(f-h)**, arrows indicate

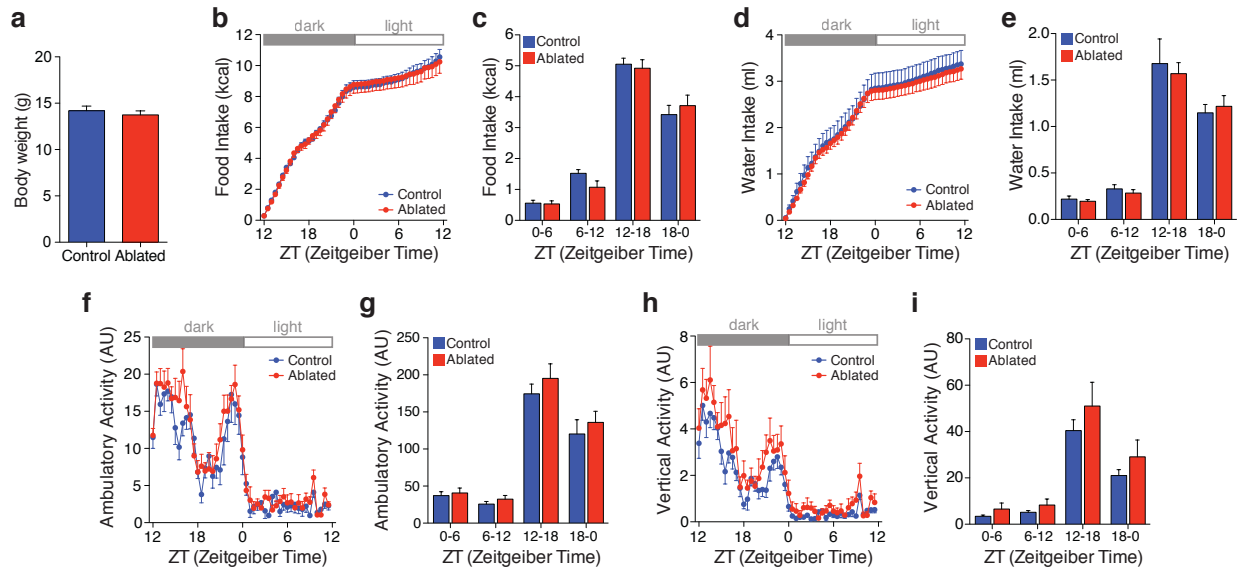
the time of stimulation (STD-LTP). In **(h)**, arrowheads indicate the time where

representative episodes are illustrated. Blue arrowheads indicate a time before the

stimulation, and red arrowheads after stimulation (LTP). Bars and symbols represent

mean \pm s.e.m.

Supplementary Figure 8:



Phenotypic characterization of control and AgRP ablated mice. A total of 8 controls and 8 AgRPDTR female mice that were injected with diphtheria toxin at postnatal age of 5 days (P5), were phenotypically characterized in their home cages. Ablation of AgRP neurons in early postnatal age (P5) did not significantly change **(a)** body weight, **(b-c)** food intake, **(d-e)** water intake, **(f-g)** ambulatory activity, and **(h-i)** vertical activity when compared to littermate control mice.

Supplementary Table 1:

	Control (n = 9)	AgRP-Sirt1 KO (n = 8)
Leptin (ng/ml)	3.86 ± 0.55	2.33 ± 0.29*
Fat mass (g)	3.94 ± 0.20	3.00 ± 0.17**
Fat (%)	17.45 ± 0.83	13.24 ± 0.81**

* $P < 0.05$.

* $P < 0.01$.

Supplementary Table 2:

Data from the analysis of electron microscopic pictures of TH positive cells in the ventral tegmental area of the midbrain from control and AgRP-Sirt1 KO adult female mice.

	Control (n = 33 cells/5 mice)	AgRP-Sirt1 KO (n = 33 cells/5 mice)	P value
Average area (μm^2):			
Cell	123.67 \pm 5.50	122.07 \pm 5.41	0.836
Nucleus	57.19 \pm 3.51	58.12 \pm 2.97	0.841
Cytosol	66.48 \pm 4.33	63.95 \pm 3.96	0.668
Ratio nucleus/cell area	0.468 \pm 0.022	0.478 \pm 0.018	0.731
Cell perimeter (μm)	46.25 \pm 1.48	47.27 \pm 1.29	0.603
Synaptic density (number of synapses per 100 μm perikarya):			
Asymmetric	1.54 \pm 0.31	1.75 \pm 0.37	0.675
Symmetric	5.80 \pm 0.71	5.62 \pm 0.62	0.851
Total	7.34 \pm 0.90	7.37 \pm 0.83	0.982
Mitochondria number:			
Number per cell area	0.346 \pm 0.016	0.341 \pm 0.019	0.840
Number per cytosol area	0.661 \pm 0.026	0.653 \pm 0.029	0.841